Saudi Journal of Biological Sciences xxx (2018) xxx–xxx

Contents lists available at ScienceDirect

Saudi Journal of Biological Sciences

journal homepage: www.sciencedirect.com

Original article

Influence of strong bases on the synthesis of silver nanoparticles (AgNPs) using the ligninolytic fungi *Trametes trogii*

Jesica María Kobashigawa [a,b], Carolina Analía Robles [a,*], María Luz Martínez Ricci [c], Cecilia Cristina Carmarán [a,b,*]

[a] Universidad de Buenos Aires, Facultad de Ciencias Exactas y Naturales, Departamento de Biodiversidad y Biología Experimental, Ciudad Autónoma de Buenos Aires C1428 EHA, Argentina
[b] CONICET-Universidad de Buenos Aires, Instituto de Micología y Botánica (INMIBO), Ciudad Autónoma de Buenos Aires C1428 EHA, Argentina
[c] CONICET-Universidad de Buenos Aires, Facultad de Ciencias Exactas y Naturales, INQUIMAE, Laboratorio de Superficies y Materiales Funcionales, Ciudad Autónoma de Buenos Aires C1428 EHA, Argentina

ARTICLE INFO

Article history:
Received 14 June 2018
Revised 10 September 2018
Accepted 18 September 2018
Available online xxxx

Keywords:
Trametes trogii
Silver nanoparticles
Green synthesis
High pH

ABSTRACT

Silver nanoparticles (AgNPs) were biosynthesized using fungal extract of *Trametes trogii*, a white rot basidiomycete involved in wood decay worldwide, which produces several ligninolytic enzymes. According to previous studies using fungi, enzymes are involved in nanoparticles synthesis, through the so-called green synthesis process, acting as reducing and capping agents. Understanding which factors could modify nanoparticles' shape, size and production efficiency is relevant. The results showed that under the protocol used in this work, this strain of *Trametes trogii* is able to synthesize silver nanoparticles with the addition of silver nitrate ($AgNO_3$) to the fungal extract obtained with an optimal incubation time of 72 h and pH 13, using NaOH to adjust pH. The progress of the reaction was monitored using UV–visible spectroscopy and synthesized AgNPs was characterized by scanning electron microscope (SEM), through in-lens and QBDS detectors, and energy-dispersive X-ray spectroscopy (EDX). Additionally, SPR absorption was modeled using Mie theory and simple nanoparticles and core-shell configurations were studied, to understand the morphology and environment of the nanoparticles. This protocol represents a simple and cheap synthesis in the absence of toxic reagents and under an environmentally friendly condition.

1. Introduction

Nanotechnology of metal nanoparticles (NPs) is nowadays a highly studied area because of their unusual optical, chemical, photoelectrochemical and electronic properties, particularly in noble metals such as silver, gold and copper (Zonooz and Salouti, 2011). The nanoscale boundary effect introduces abnormal properties that are remarkably different from bulk metals often resulting from enhanced surface interactions or quantum confinement (Scholl et al., 2012). When the frequency of an incident electromagnetic field matches the natural frequency of surface electrons oscillating, a strong absorption peak appears as a consequence of a surface plasmon resonance (SPR) in the visible-light range (Linic et al., 2015; Maier, 2007; Wu et al., 2015). The analysis of the SPR enables a characterization of the morphology and size of the metal NPs (Noguez, 2007). Particularly, silver nanoparticles (AgNPs) are extensively used in several fields of biotechnology and have applications in different areas like medicine, agriculture, electronic industry and others (Li et al., 2005; Prabhu and Poulose, 2012).

Chemical methods of synthesis of nanoparticles are widely used but they usually make use of several chemical compounds that are harmful to the environment (Punjabi et al., 2015). In contrast, green methods using biological organisms like bacteria, plants and fungi as promoters for the synthesis of nanoparticles are

* Corresponding authors at: Universidad de Buenos Aires, Facultad de Ciencias Exactas y Naturales, Departamento de Biodiversidad y Biología Experimental, Ciudad Autónoma de Buenos Aires C1428 EHA, Argentina (C.A. Robles and C.C. Carmarán).
E-mail addresses: j.kobashigwa@bg.fcen.uba.ar (J.M. Kobashigawa), cararobles@bg.fcen.uba.ar (C.A. Robles), mricci@qi.fcen.uba.ar (M.L. Martínez Ricci), carmaran@bg.fcen.uba.ar (C.C. Carmarán).

Peer review under responsibility of King Saud University.

Production and hosting by Elsevier

https://doi.org/10.1016/j.sjbs.2018.09.006
1319-562X/

emerging as an important branch of nanotechnology, due to their eco-friendly, safe, and cost-effective nature (Gajbhiye et al., 2009; Ghorbani et al., 2015; Honary et al., 2012; Korbekandi et al., 2013; Kuppusamy et al., 2016; Matinise et al., 2017; Sone et al., 2015). Although in recent years the popularity of the biological synthesis of NPs has been increasing, lack of knowledge prevents these green methods to match chemical synthesis quality. Nowadays, the production of nanoparticles using biological organisms presents as a challenge for obtaining monodisperse nanoparticles and understanding which factors could modify their shape, size and production efficiency. Among these factors, temperature, precursor concentration and ions presence have been mentioned (Abdel-Hafez et al., 2016; Filankembo and Pileni, 2000; Gade et al., 2014).

Fungi known as "white-rot fungi" (also ligninolytic fungi) are widely used for bioremediation due to their ability to transform or mineralize a wide range of environmentally hazardous compounds, because of the large amount of enzymes they release to the environment Baker and Satish, 2012). In addition, these fungi have been studied as promoters of the synthesis of nanoparticles due to their high biomass production and easy handling (Cuevas et al., 2015; Durán et al., 2014; Paul et al., 2015; San Chan and Don, 2013). Species of the genus *Trametes* Fr. encompass polyporoid white rot fungi widely distributed in various biotopes, having been the subject of many physiological and biochemical studies (Tomšovský et al., 2006), and are considered very good laccase producers (Gorshina et al., 2006). Durán et al. (2014) obtained silver nanoparticles using laccase enzyme extracted from a member of this genus, *Trametes versicolor* (L.) Lloyd. Another species of the genus, *Trametes trogii* Berk, is considered as a good producer of ligninases, with the ability to degrade several hazardous compounds (Levin et al., 2003). These characteristics indicate this species' eligibility for nanoparticles synthesis. Silver nanoparticles have a high demand for industrial and clinical purposes, the development of environmental friendly procedures for AgNPs synthesis appears as a good starting point for the evaluation of the ability of *T. trogii* in their synthesis. In our knowledge the ability of *T. trogii* to produce metallic nanoparticles has not yet been tested.

In this work we tested the ability of native *Trametes trogii* to synthesize AgNPs. We characterized their formation over time by studying their absorption spectrum in the UV–vis range and their morphology by scanning electron microscope (SEM). Additionally, the effect of NaOH and KOH over the synthesis of AgNPs was evaluated. The NPs composition was verified through Energy-Dispersive X-ray spectra (EDX) analysis.

2. Materials and methods

2.1. Chemical compounds

Silver nitrate ($AgNO_3$, Sigma Aldrich) 100 mM was used for the biosynthesis of Ag nanoparticles. KOH (1 M) and NaOH (1 M) were used to adjust pH.

2.2. Microorganism for the biosynthesis of nanoparticles

A native strain of *Trametes trogii* (BAFCcult 463) was used in all the assays. The strain was incubated in malt extract agar 2% (MEA) plates, at 24 °C for 15 days before being used for the inoculum preparation.

2.3. Growth curve of Trametes trogii

Erlenmeyer flasks containing 100 mL of growth medium were used. Growth medium was composed of 15 g L^{-1} glucose, 5 g L^{-1} potato peptone, and 25 g L^{-1} yeast extract. The medium was sterilized, inoculated with 5 mm plugs of the strain and incubated for 24 days at 100 rpm and 28 °C in the dark. The mycelium was harvested every 2 days from day 3 to day 21, filtered through a filter paper using a Büchner funnel and dried overnight at 70 °C. Then the dry weight of mycelia was determined.

2.4. Biosynthesis of silver nanoparticles and kinetic analysis

An essay was performed using the same growth medium and conditions as in 2.3, but, in this case, the incubation time lasted 5 days. The fungal biomass obtained at the end of the incubation period was filtered through a Büchner funnel and washed thoroughly with sterile distilled water to remove the traces of media components. Filtered mycelium was then transferred into 100-mL Erlenmeyer flasks containing 50 mL sterile distilled water and incubated in an orbital shaker (100 rpm) for 48 hs at 28 °C. After 48 hs the suspension was filtered through a Büchner funnel, mycelium was separated and the mycelium-free fungal filtrate (hereafter, fungal filtrate) was used for synthesis of AgNPs.

For the biosynthesis of AgNPs, the fungal filtrate (pH 8) was used. $AgNO_3$ 100 mM was added to obtain a final concentration of 5 mM and then incubated for 20 days on an orbital shaker (100 rpm) at 28 °C in the dark. Later, the same procedure was performed on the fungal filtrate but increasing the pH from 8 to 13, with either NaOH 1 M or KOH 1 M, and incubated for 5 days. Aliquots containing only the fungal filtrate (pH 8), without the salt (control 1), and flasks containing sterile distilled water with the salt (control 2). All the treatments were performed in triplicate.

Additionally, in order to evaluate the kinetics of the AgNPs, samples were prepared with NaOH: pH 13, 100 rpm, 28 °C, 5 mM of $AgNO_3$. After the addition of the salt, a 1-mL aliquot was removed from each flask on days 0 (*to*), 1, 2, 3 and 8 for later characterization and analysis.

2.5. Characterization of silver nanoparticles

To detect the biosynthesis of silver nanoparticles UV–visible spectra were obtained using a spectrophotometer Shimadzu UV-MINI 1240 (Tokyo, Japan) by scanning the absorbance spectra in 200–800 nm range of wavelength.

Nanoparticles obtained were characterized using a scanning electron microscope (SEM) model Zeiss SUPRA TM 40 (Oberkochen, Germany), through the detector in-lens (SE) at 20 kV accelerating voltage. For the kinetic analysis, the nanoparticles silver core was also characterized adding a quadrant back-scattered electron detector (QBSD). In the obtained images, "brighter" intensity areas of QBSD images correlate with greater average Z (atomic number) in the sample, and "darker" areas correspond to lower average Z revealing the presence of silver in the sample, omitting the carbon compounds. This technique entails lower resolution images. Spectrum was measured at 10 kV accelerating voltage. EDX was done to determine nanoparticleś composition.

2.6. Size frequency

Approximate particle sizes were obtained using the ImageJ 1.49v (National Institutes of Health, USA) over the QBSD images obtained on day 8 (core analysis) registering the frequency of particle size in samples.

2.7. Modeling

Surface plasmon resonance (SPR) absorption was modeled for day 8 polydisperse sample using Mie theory (Bohren and Huffman, 2008; van de Hulst, 1957). Simple nanoparticles and

Please cite this article in press as: Kobashigawa, J.M., et al. Influence of strong bases on the synthesis of silver nanoparticles (AgNPs) using the ligninolytic fungi *Trametes trogii*. Saudi Journal of Biological Sciences (2018), https://doi.org/10.1016/j.sjbs.2018.09.006

core-shell configurations were studied to understand the morphology and environment of the silver nanoparticles.

3. Results and discussion

3.1. Growth curve of Trametes trogii

The growth curve of *T. trogii* (Fig. 1) showed that between days 3 and 14 the fungus was in the initial state of latency. Then, between days 14 and 21, an exponential growth phase was observed. Similar results were reported by Levin et al. (2010). Taking into account that the incubation time for nanoparticles synthesis in the present work was five days (see arrow), the metabolites responsible for biosynthesis of NPs were produced in the latent phase.

3.2. Biosynthesis of silver nanoparticles

No evidence of AgNPs synthesis was observed when $AgNO_3$ was added directly to the fungal filtrate (pH 8), after 20 days (data not shown). It is known that in alkaline pH, the Zeta potential value of AgNPs tends to be higher than in acidic pH, and nanoparticles are relatively more stable due to the electrostatic repulsion derived from the adsorption of OH^- on AgNPs, while at acidic pH, aggregates are formed due to unavailability of OH^- ions and show low value of zeta potential (Birla et al., 2013). In Fig. 2 it is shown the UV–Vis spectrum from the treated (KOH or NaOH) fungal filtrate at pH 13 after 5 days of incubation, which exhibits a peak around 430 nm, which indicated the presence of metallic nanoparticles (Birla et al., 2013; Khlebtsov and Dykman, 2010; Slistan-Grijalva et al., 2005). Also the biosynthesis of NPs was detected by visual observation of the characteristic color change, a yellowish-brown color in the solution associated to an attributable SPR band of AgNPs. There was not a noticeable difference between the treatment with KOH and NaOH. To perform the measurements, dilutions had to be made because the high concentration of the solution saturated the spectrophotometer. These results agree with previous reports from Birla et al. (2013), indicating that alkaline solutions promote the synthesis of NPs. Samples exhibited an important absorption band at low wavelength region (around 265 nm) which were attributed to aromatic amino acids of proteins (Honary et al., 2012). Control solutions neither developed the brown color nor displayed the characteristic band (Fig. 2) (data not shown for control 2). No differences were detected in AgNPs solutions which maintained their brownish colour and present the same SPR absorbance intensity with no precipitation after 4 months (data not shown).

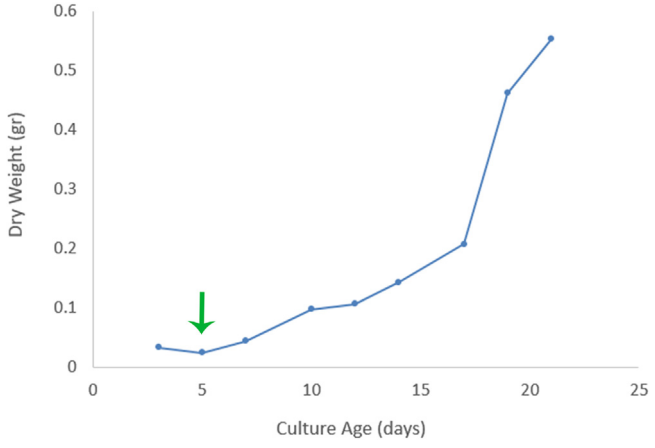

Fig. 1. Growth curve of *Trametes trogii* under the following conditions: growth medium composed of 15 g L^{-1} glucose, 5 g L^{-1} potato peptone, and 25 g L^{-1} yeast extract, 80 rpm and 28 °C in the dark. The arrow indicates the day of the start of the silver nanoparticle biosynthesis.

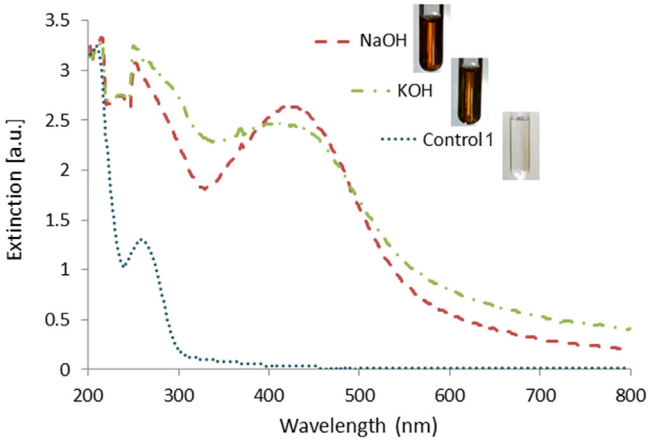

Fig. 2. Extinction spectrum of samples treated with AgNO3 (5 mM) and NaOH or KOH, and fungal filtrate control 1. Dilution 1:2. A strong, broad peak located at around 430 nm was observed in the spectra. Insets show visual results corresponding to each treatment.

3.3. Characterization of silver nanoparticles

Fig. 3 shows SEM images of the obtained NPs for NaOH (Fig. 3a) and KOH (Fig. 3b) synthesis. NPs in clusters are observed, this arrangement could be an artifact of the mounting process, for instance when the colloid of NPs is dried, agglomeration occurs, forming clusters as seen in the images. Similar images of the clustering of NPs were reported by Durán et al. (2005). The images only exhibit the organic compounds that surround the metallic NPs. In fact, the EDX spectrum (Fig. 3c and d) revealed the presence of pure metallic silver NPs, showing a peak at approximately 3 keV which correspond s to Ag (Abdel-Hafez et al., 2016).

3.4. Kinetic analysis

The obtained results showed that the absorbance intensity caused by the AgNPs plasmon increased over the incubation time. The first steps in the nanoparticle formation were detected after 12 h. As Fig. 4 shows, the plasmonic band initiated on day 1, but the results revealed that the rate of AgNPs formation increased substantially between days 2 and 3. The maximum reduction of Ag^+ ions into Ag^0 was obtained after 8 days showing a peak center displacement toward low wavelengths of approx 15 nm in comparison with day 3 spectra, although maximum absorbance peak differed little from day 8 respect to day 3. Control samples showed no peak in the spectrum (data not shown). The capping formation could explain this plateau behaviour, since it limits not only the particle size but also the reducing power of the fungal strain. Taking into account the complexity of this biological system it is difficult to elucidate the involved mechanisms.

Under the conditions of the present study, 72 h would be the optimal incubation period in terms of efficiency of the biosynthesis process as a function of time. As other previous studies (Slistan-Grijalva et al., 2005), the bandwidth of the plasmon obtained would indicate polydispersity in the nanoparticles so the conditions tested in this work has not allowed to obtain monodisperse nanoparticles. However, our results differ in the analysis of the nanoparticles formation period, taking into account the differences about fungal source, incubation media, growing conditions, etc.

Please cite this article in press as: Kobashigawa, J.M., et al. Influence of strong bases on the synthesis of silver nanoparticles (AgNPs) using the ligninolytic fungi *Trametes trogii*. Saudi Journal of Biological Sciences (2018), https://doi.org/10.1016/j.sjbs.2018.09.006

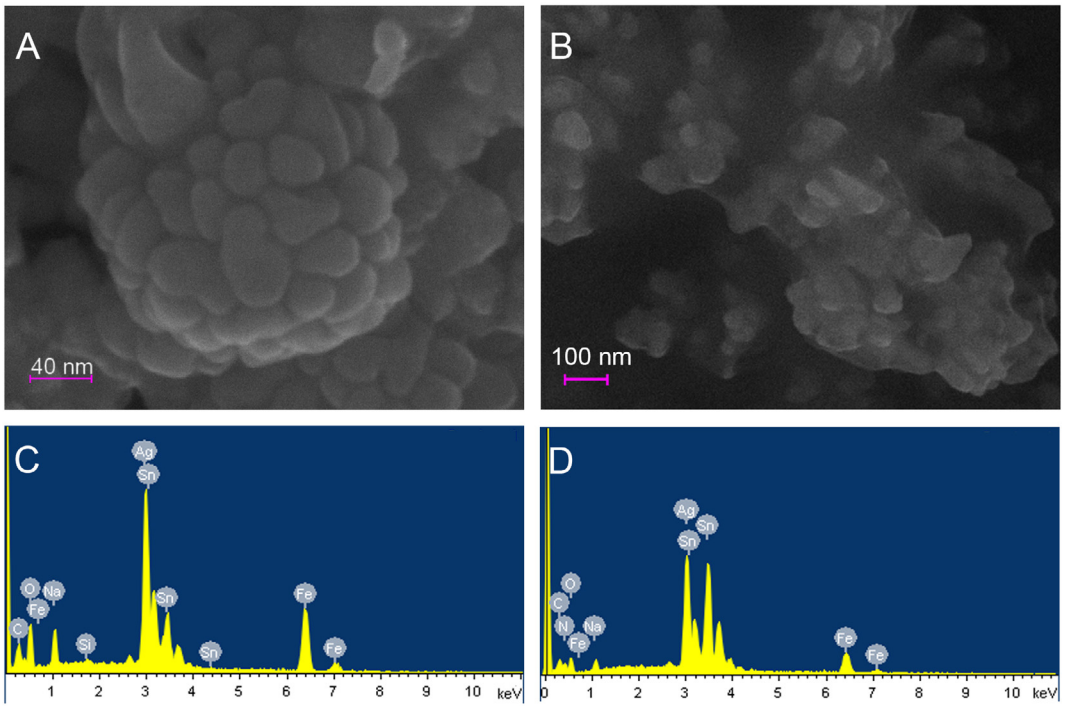

Fig. 3. A–B. Scanning electron micrographs (in-lens detector, EHT = 20 kV) of aggregated and capped silver nanoparticles and spherical silver nanoparticles using NaOH (A) or KOH (B). C–D. EDX spectrum of biosynthesized AgNPs using NaOH (C) or KOH (D). Sn, Fe and Si peaks correspond to the wafer that supports the sample.

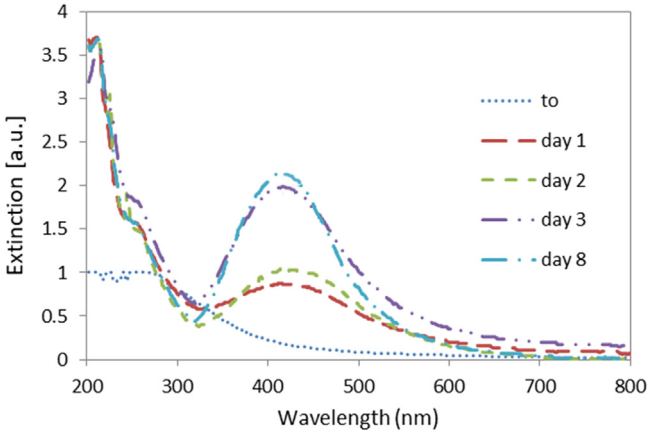

Fig. 4. Kinetics of the extinction on resonance plasmon absorption (SPR) based on the UV–visible spectrum of silver nanoparticles. $AgNO_3$ 5 mM. Dilution 1:10. Broad peak located at around 415–430 was observed in the treated samples.

(Abdel-Hafez et al., 2016; Ahmad et al., 2003; Birla et al., 2013; Gade et al., 2014; Korbekandi et al., 2013).

3.5. Characterization and modeling of nanoparticles

As in Fig. 3c and d, the EDX spectrum (data shown in Supplementary Fig. 1) for the kinetic study confirmed the metallic composition of AgNPs. The SEM images in Fig. 5 were obtained from the SE detector and showed that AgNPs present an organic capping that was not visible in the QBSD images. Some of the images of the present study suggest that NPs have a spherical structure, while others suggest that NPs would have elongated or rod forms (days 1, 2 and 3). In many cases NPs appeared clustered. Khlebtsov and Dykman (2010) reported two peaks of extinction from rods NPs (nanorods) that vary according to the aspect ratio of the NP axis: one corresponding to the cross section and another to the longitudinal section of the nanorod. However, in our extinction results the presence of a single peak of plasmonic band absorption was observed, which infers spherical, core-shell, ellipsoidal AgNPs of low eccentricity.

The proportion of non-spherical NPs is markedly lower respect to spherical ones, hence the absorbance of the plasmonic bands is not observed in the extinction spectrum (Ojha et al., 2013). Recently studies performed by Razumova et al. (2018a, b) indicate that very clean conditions are needed for the formation of non-spherical NPs, which cannot be performed using biological organisms. Another possible explanation for the absence of more than one plasmonic absorption peak, is that the reduction of the ion is mediated by polymers and the spheric nanoparticles are probably aligned appearing as nanorods. The "nanorods" were not recognized in the samples of day 8. It is possible that at the beginning of the reaction, nanorods are formed but later they derive in separated spherical nanoparticles. To our knowledge, there are no reports of rod-shaped silver nanoparticles in the literature of biological synthesis.

In order to have a better understanding of the system under study, Mie theory (Mätzler, 2002) was used to model the extinction of day 8 spectra. For a bare spherical metallic Ag NP, surrounded by an aqueous solution, the plasmonic band center is expected at $\lambda_{SPR} \cong 385$ nm which is not coincident with the one observed in Fig. 4.

To explain this difference, a polydisperse core-shell NP distribution has been considered. This proposed model is based on two main aspects: polydispersity has been considered since the amplitude and wavelength position of the plasmonic band depends on the metallic NP size and consequently, some authors associate shorter wavelengths to the presence of smaller NPs and longer wavelengths to polydisperse and larger NPs (Hamedi et al., 2014). Fig. 6 shows a complete characterization of the size frequency of day 8. During the measurement, those NPs close to clusters showed larger sizes than those that were single. When

Please cite this article in press as: Kobashigawa, J.M., et al. Influence of strong bases on the synthesis of silver nanoparticles (AgNPs) using the ligninolytic fungi *Trametes trogii*. Saudi Journal of Biological Sciences (2018), https://doi.org/10.1016/j.sjbs.2018.09.006

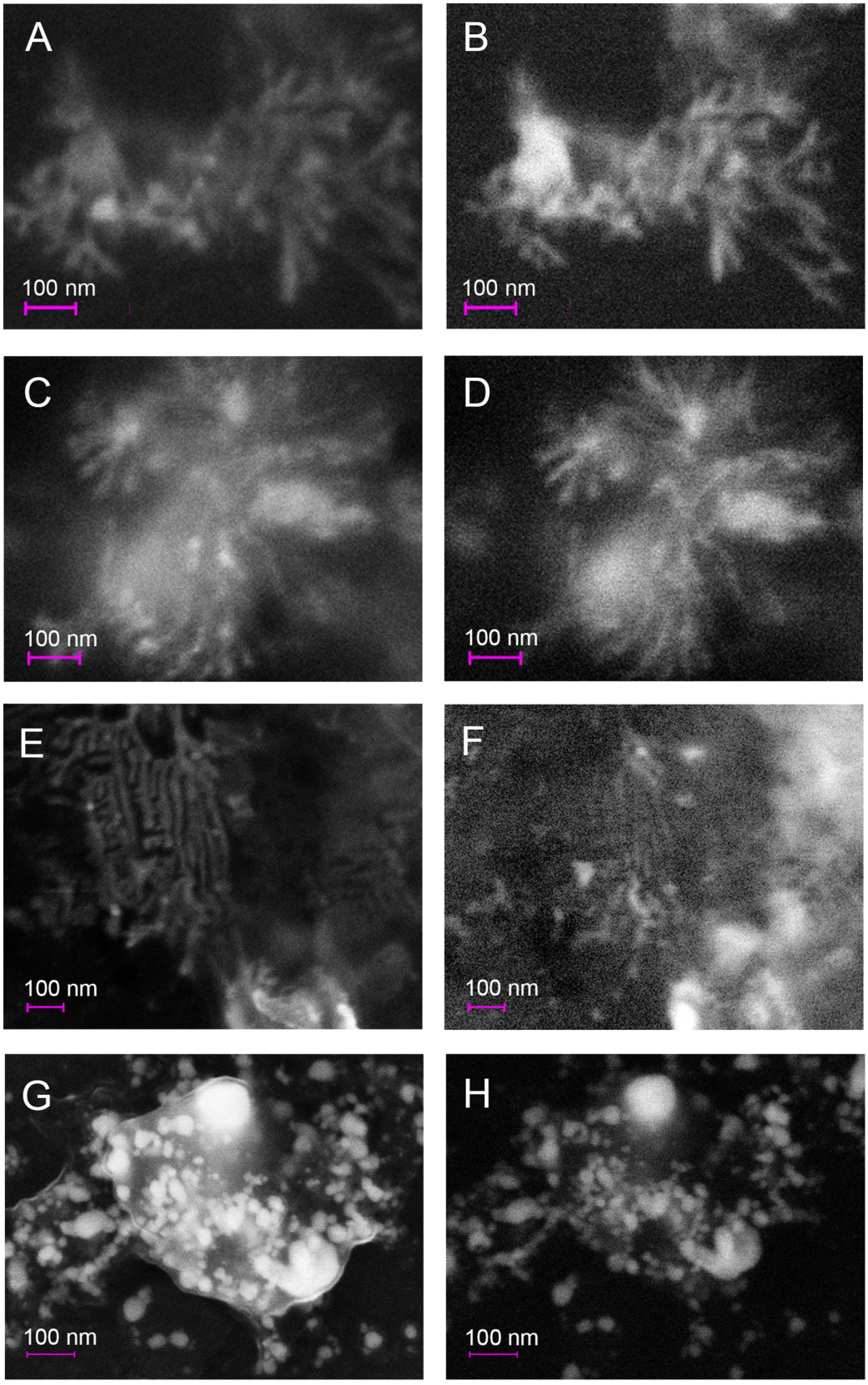

Fig. 5. Scanning electron micrographs comparing, in the same area, the in-Lens detector (A, C, E, G) and the QBSD detector (B, D, F, H) (EHT = 10 kV). A-B: day 1. C-D: day 2. E-F: day 3. G-H: day 8.

analyzing the kinetic of the synthesis of silver nanoparticles in the present work, it was noticed that between days 1 and 3 there was a decrease in the peak of the order of 9 nm, which would imply that the NPs acquire a greater monodisperse character over time.

Please cite this article in press as: Kobashigawa, J.M., et al. Influence of strong bases on the synthesis of silver nanoparticles (AgNPs) using the ligninolytic fungi *Trametes trogii*. Saudi Journal of Biological Sciences (2018), https://doi.org/10.1016/j.sjbs.2018.09.006

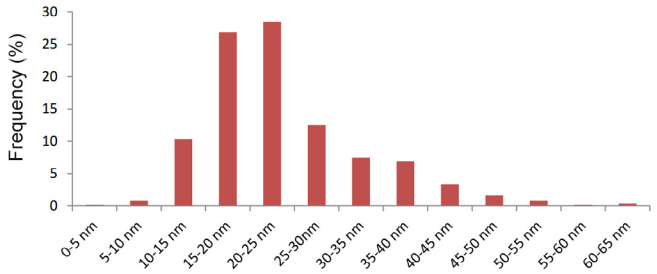

Fig. 6. Frequency distribution of AgNPs sizes.

The core-shell configuration geometry, as the one schemed in Fig. 7a, has been selected as a consequence of the SEM images of Fig. 3 where an organic capping has been observed. The SPR peak center in this configuration is typically red shifted (Santillán et al., 2011) respect to the value obtained in the Frölich condition for a bare metallic NP. This red shift could have been also explained by spheroids of notorious eccentricity (Kelly et al., 2003) taking into account the depolarizing factors, however, micrographs (Figs. 3 and 5g, h) do not exhibit this type of geometry but a core-shell one.

With these two considerations, a complete modeling has been made in Fig. 7b for day 8 where Mie theory for core-shell NPs has been applied for each of the sizes and pondered by the size frequency information obtained in Fig. 6. Two different optical properties have been considered for the shell modeling and compared with the experimental extinction spectrum. When the shell's refractive index is considered as a strictly dielectric media, no imaginary component should be considered for the shell's refractive index ($nshell \in \Re$) (see Supplementary Material for specific modeling data). In this case, the modeled extinction spectra clearly differed from the experimental one as in parameters as the FWHM (Full Width at Half Maximum) and also the SPR absorption peak position.

However, when shell's refractive index is considered complex ($\mathrm{Im}\,(nshell) \neq 0$), the extinction spectra well matches the experimental one. The FWHM increases and the SPR peak red shifts toward the experimental value. A not zero imaginary component in the shell refractive index, simply implies that the shell media has absorbing properties. For the case of study under consideration, the reason would probably be an oxidation processes round the metallic core which could result in the presence of some species like Ag_2O (which has complex refractive index (Qiu et al., 2005) when the metal is exposed to an oxygen atmosphere ($4Ag + O2 \rightarrow 2Ag2O$). The slow differences among the experimental and modeled spectra can be due to the before mentioned low eccentricity rods or ellipsoids (see SI-Section 2 for specific modeling data).

Several studies have reported that the synthesis of nanoparticles would be related to the action of the enzymes that the fungi secrete into the medium (Ahmad et al., 2002; Kumar et al., 2007). Durán et al. (2014) studied the production of AgNPs by *Trametes versicolor* and suggested that the main pathway involved was the interaction of silver ions with the T1 site of laccase, producing silver nanoparticles with the concomitant inactivation of laccase activity and posterior complexing with silver ions. These authors additionally suggested the direct interaction of silver ions with the Cys-Cys moiety and the sulfhydryl moiety bound laccase to silver nanoparticles as capped proteins. Levin et al. (2002), studying copper induction of lignin-modifying enzymes in the white-rot fungus *Trametes trogii* (BAFCult 463), the same fungal strain used in the present study, reported an optimum pH for laccase activity as 3.4, and although the enzyme was active over a wider range of pH values, its activity was negligible above pH 5. The optimum temperature for laccase activity was 50 °C. At 30 °C and 60 °C relative laccase activity was approximately 85% of its maximum, and laccase activity was 76% of its maximum at 70 °C. An alkaline pH, as the pH used in the present work, usually involves denaturation of the proteins, including laccase enzyme. Taking into account the available data and the assays conditions used here, it is not clear how an inactive and denatured laccase could impact on the synthesis of silver NPs, and if the capping observed could be explained by the interaction with the Cys-Cys moiety and the sulfhydryl moiety. Therefore, more studies should be performed to ascertain the role of the laccase in the synthesis of silver nanoparticles.

4. Conclusions

Nanotechnology is currently a subject of active development and the synthesis of NPs is a widely studied area due to the diverse and potential applications that these particles have in various fields (Park et al., 2016). The study of the biosynthesis of NPs from

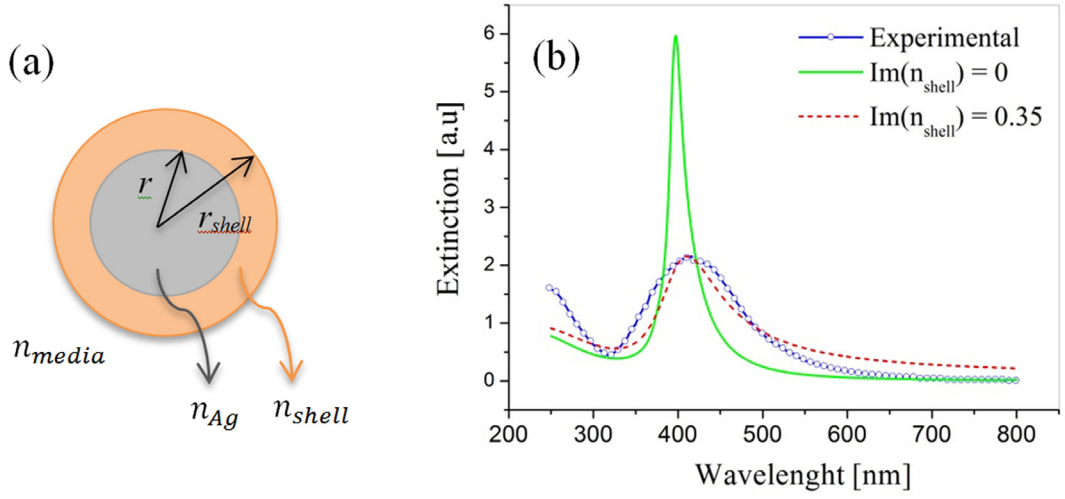

Fig. 7. (a) Core-shell configuration geometry used for modeling. (b) Comparison between experimental extinction (blue circles) spectra for day 8 biosynthesis with core-shell modeling considering a dielectric shell (green solid line) or an absorbing shell (red dashed line). (For interpretation of the references to colour in this figure legend, the reader is referred to the web version of this article.)

Please cite this article in press as: Kobashigawa, J.M., et al. Influence of strong bases on the synthesis of silver nanoparticles (AgNPs) using the ligninolytic fungi *Trametes trogii*. Saudi Journal of Biological Sciences (2018), https://doi.org/10.1016/j.sjbs.2018.09.006

ligninolytic fungi, however, is a less studied subject (Cuevas et al., 2015). This work represents a contribution to the study of the capacity of synthesis of AgNPs by fungi, using the ligninolytic fungi *Trametes trogii*. The results showed that under the protocol used, *T. trogii* is able to synthesize silver nanoparticles from the fungal filtrate, adding $AgNO_3$ (5 mM), at pH 13, with an optimal incubation time of 72 hs.

The results show that a high pH is conducive to the synthesis of AgNPs working with this biological organism. Several authors have suggested enzymes might be responsible for the reduction of the metal ion, therefore a better study of the enzymatic profile of this fungi is necessary to determine which enzymes have a good performance at high pH.

Conflicts of interest

The authors declare no conflicts of interest.

Acknowledgments

This study was supported by the CONICET [PIP 112 20150100956], National Agency for Science and Technology Promotion (ANPCyT) [PICT N° 2015-1038], University of Buenos Aires [UBACYT 20020150100067BA, UBACYT 20020170200298BA].

Appendix A. Supplementary material

Supplementary data to this article can be found online at https://doi.org/10.1016/j.sjbs.2018.09.006.

References

Abdel-Hafez, S.I., Nafady, N.A., Abdel-Rahim, I.R., Shaltout, A.M., Mohamed, M.A., 2016. Biogenesis and optimisation of silver nanoparticles by the endophytic fungus *Cladosporium sphaerospermum*. Int. J. Nano Chem. 2, 11–19.

Ahmad, A., Mukherjee, P., Mandal, D., Senapati, S., Khan, M.I., Kumar, R., Sastry, M., 2002. Enzyme mediated extracellular synthesis of CdS nanoparticles by the fungus, *Fusarium oxysporum*. J. Am. Chem. Soc. 124, 12108–12109.

Ahmad, A., Mukherjee, P., Senapati, S., Mandal, D., Khan, M.I., Kumar, R., Sastry, M., 2003. Extracellular biosynthesis of silver nanoparticles using the fungus *Fusarium oxysporum*. Colloids Surf. B 28, 313–318.

Baker, S., Satish, S., 2012. Endophytes: toward a vision in synthesis of nanoparticle for future therapeutic agents. Int. J. Bio-Inorg. Hybd. Nanomat. 1, 67–77.

Birla, S.S., Gaikwad, S.C., Gade, A.K., Rai, M.K., 2013. Rapid synthesis of silver nanoparticles from *Fusarium oxysporum* by optimizing physicocultural conditions. Sci. World J. 12.

Bohren, C.F., Huffman, D.R., 2008. Absorption and Scattering of Light by Small Particles. John Wiley & Sons, New York.

Cuevas, R., Durán, N., Diez, M.C., Tortella, G.R., Rubilar, O., 2015. Extracellular biosynthesis of copper and copper oxide nanoparticles by *Stereum hirsutum*, a native white-rot fungus from chilean forests. J. Nanomater. 16, 57.

Durán, N., Cuevas, R., Cordi, L., Rubilar, O., Diez, M.C., 2014. Biogenic silver nanoparticles associated with silver chloride nanoparticles (Ag@ AgCl) produced by laccase from *Trametes versicolor*. Springer Plus 3, 645.

Durán, N., Marcato, P.D., Alves, O.L., De Souza, G.I., Esposito, E., 2005. Mechanistic aspects of biosynthesis of silver nanoparticles by several *Fusarium oxysporum* strains. J. Nanobiotechnol. 3, 8.

Filankembo, A., Pileni, M.P., 2000. Is the template of self-colloidal assemblies the only factor that controls nanocrystal shapes? J. Phys. Chem. B 104, 5865–5868.

Gade, A., Gaikwad, S., Duran, N., Rai, M., 2014. Green synthesis of silver nanoparticles by *Phoma glomerata*. Micron 59, 52–59.

Gajbhiye, M., Kesharwani, J., Ingle, A., Gade, A., Rai, M., 2009. Fungus-mediated synthesis of silver nanoparticles and their activity against pathogenic fungi in combination with fluconazole. Nanomedicine: Nanotechnology. Biol. Med. 5, 382–386.

Ghorbani, H.R., Mehr, F.P., Poor, A.K., 2015. Extracellular synthesis of copper nanoparticles using culture supernatants of *Salmonella typhimurium*. Orient. J. Chem. 31, 527–529.

Gorshina, E.S., Rusinova, T.V., Biryukov, V.V., Morozova, O.V., Shleev, S.V., Yaropolov, A.I., 2006. The dynamics of oxidase activity during cultivation of basidiomycetes from the genus *Trametes* Fr. Appl. Biochem. Microbiol. 42, 558–563.

Hamedi, S., Shojaosadati, S.A., Shokrollahzadeh, S., Hashemi-Najafabadi, S., 2014. Extracellular biosynthesis of silver nanoparticles using a novel and non-pathogenic fungus, *Neurospora intermedia*: controlled synthesis and antibacterial activity. World J. Microbiol. Biotechnol. 30, 693–704.

Honary, S., Barabadi, H., Gharaei-Fathabad, E., Naghibi, F., 2012. Green synthesis of copper oxide nanoparticles using *Penicillium aurantiogriseum*, *Penicillium citrinum* and *Penicillium waksmanii*. Dig. J. Nanomater. Bios. 7, 999–1005.

Kelly, K.L., Coronado, E., Zhao, L.L., Schatz, G.C., 2003. The optical properties of metal nanoparticles: the influence of size, shape, and dielectric environment. J. Phys. Chem. B 107, 668–677.

Khlebtsov, N.G., Dykman, L.A., 2010. Optical properties and biomedical applications of plasmonic nanoparticles. J. Quant. Spectrosc. Radiat. Transfer. 111, 1–35.

Korbekandi, H., Ashari, Z., Iravani, S., Abbasi, S., 2013. Optimization of biological synthesis of silver nanoparticles using *Fusarium oxysporum*. Iran J. Pharm. Res. 12, 289–298.

Kumar, S.A., Abyaneh, M.K., Gosavi, S.W., Kulkarni, S.K., Pasricha, R., Ahmad, A., Khan, M.I., 2007. Nitrate reductase-mediated synthesis of silver nanoparticles from AgNO3. Biotechnol. Lett. 29, 439–445.

Kuppusamy, P., Yusoff, M.M., Maniam, G.P., Govindan, N., 2016. Biosynthesis of metallic nanoparticles using plant derivatives and their new avenues in pharmacological applications–An updated report. Saudi Pharm. J. 24, 473–484.

Levin, L., Forchiassin, F., Ramos, A.M., 2002. Copper induction of lignin-modifying enzymes in the white-rot fungus *Trametes trogii*. Mycologia 94 (3), 377–383.

Levin, L., Melignani, E., Ramos, A.M., 2010. Effect of nitrogen sources and vitamins on ligninolytic enzyme production by some white-rot fungi. Dye decolorization by selected culture filtrates. Bioresour. Technol. 101, 4554–4563.

Levin, L., Viale, A., Forchiassin, A., 2003. Degradation of organic pollutants by the white rot basidiomycete *Trametes trogii*. Int. Biodeterior. Biodegrad. 52, 1–5.

Li, Y., Wu, Y., Ong, B.S., 2005. Facile synthesis of silver nanoparticles useful for fabrication of high-conductivity elements for printed electronics. J. Am. Chem. Soc. 127, 3266–3267.

Linic, S., Aslam, U., Boerigter, C., Morabito, M., 2015. Photochemical transformations on plasmonic metal nanoparticles. Nat. Mater. 14, 567–576.

Maier, S.A., 2007. Plasmonics: Fundamentals and Applications. Springer Science & Business Media, New York.

Matinise, N., Fuku, X.G., Kaviyarasu, K., Mayedwa, N., Maaza, M., 2017. ZnO nanoparticles via *Moringa oleifera* green synthesis: physical properties & mechanism of formation. Appl. Surf. Sci. 406, 339–347.

Mätzler C., 2002. MATLAB Functions for Mie Scattering and Absorption, Res. Rep. 2002-08, Inst. für Angew. Phys., Bern.

Noguez, C., 2007. Surface plasmons on metal nanoparticles: the influence of shape and physical environment. J. Phys. Chem. C 111, 3806–3819.

Ojha, A.K., Forster, S., Kumar, S., Vats, S., Negi, S., Fischer, I., 2013. Synthesis of well–dispersed silver nanorods of different aspect ratios and their antimicrobial properties against gram positive and negative bacterial strains. J. Nanobiotechnol. 11, 42.

Park, T.J., Lee, K.G., Lee, S.Y., 2016. Advances in microbial biosynthesis of metal nanoparticles. Appl. Microbiol. Biotechnol. 100, 521–534.

Paul, S., Singh, A.R., Sasikumar, C.S., 2015. Green synthesis of bio-silver nanoparticles by *Parmelia perlata*, *Ganoderma lucidum* and *Phellinus igniarius* & their fields of application. Indian J. Res. Pharm. Biotechnol. 3, 100.

Prabhu, S., Poulose, E.K., 2012. Silver nanoparticles: mechanism of antimicrobial action, synthesis, medical applications, and toxicity effects. Int. Nano Lett. 2, 32.

Punjabi, K., Choudhary, P., Samant, L., Mukherjee, S., Vaidya, S., Chowdhary, A., 2015. Biosynthesis of nanoparticles: a review. Int. J. Pharm. Sci. Rev. Res. 30, 219–226.

Qiu, J.H., Zhou, P., Gao, X.Y., Yu, J.N., Wang, S.Y., Li, J., Zheng, Y.X., Yang, Y.M., Song, Q. H., Chen, L.Y., 2005. Ellipsometric study of the optical properties of silver oxide prepared by reactive magnetron sputtering. J. Korean Phys. Soc. 46, S269–S275.

Razumova, Y.A., Toropov, N.A., Vartanyan, T.A., 2018a. Chemically synthesized silver nanorods intended for near IR applications. Proc. SPIE, Nanophoton. VII 10672, 1067233.

Razumova, Y.A., Toropov, N.A., Vartanyan, T.A., 2018b. Chemically synthesized gold and silver particles absorbing in the near-IR spectral range. Opt. Spectrosc. 124, 703–706.

San Chan, Y., Don, M.M., 2013. Biosynthesis and structural characterization of Ag nanoparticles from white rot fungi. Mater. Sci. Eng. C 33, 282–288.

Santillán, J.M.J., Scaffardi, L.B., Schinca, D.C., 2011. Quantitative optical extinction-based parametric method for sizing a single core–shell Ag–Ag_2O nanoparticle. J. Phys. D Appl. Phys. 44, 105–1104.

Scholl, J.A., Koh, A.L., Dionne, J.A., 2012. Quantum plasmon resonances of individual metallic nanoparticles. Nature 483, 421–427.

Slistan-Grijalva, A., Herrera-Urbina, R., Rivas-Silva, J.F., Ávalos-Borja, M., Castillón-Barraza, F.F., Posada-Amarillas, A., 2005. Classical theoretical characterization of the surface plasmon absorption band for silver spherical nanoparticles suspended in water and ethylene glycol. Phys. E 27, 104–112.

Sone, B.T., Manikandan, E., Gurib-Fakim, A., Maaza, M., 2015. Sm_2O_3 nanoparticles green synthesis via *Callistemon viminalis*' extract. J. Alloys Compd. 650, 357–362.

Tomšovský, M., Kolařík, M., Pažoutová, S., Homolka, L., 2006. Molecular phylogeny of European *Trametes* (Basidiomycetes, Polyporales) species based on LSU and ITS (nrDNA) sequences. Nova Hedwigia 82, 269–280.

van de Hulst, H.C., 1957. Light Scattering by Small Particles. Dover Press, New York.

Wu, D.Y., Zhang, M., Zhao, L.B., Huang, Y.F., Ren, B., Tian, Z.Q., 2015. Surface plasmon-enhanced photochemical reactions on noble metal nanostructures. Sci. China: Chem. 58, 574–585.

Zonooz, N.F., Salouti, M., 2011. Extracellular biosynthesis of silver nanoparticles using cell filtrate of *Streptomyces* sp. ERI-3. Sci. Iran 18, 1631–1635.

Please cite this article in press as: Kobashigawa, J.M., et al. Influence of strong bases on the synthesis of silver nanoparticles (AgNPs) using the ligninolytic fungi *Trametes trogii*. Saudi Journal of Biological Sciences (2018), https://doi.org/10.1016/j.sjbs.2018.09.006